PHYSICAL REVIEW B VOLUME 7, NUMBER 1 1 JANUARY 1973

Temperature-Dependent Hyperfine Interactions in Fe_2B†*

Kenneth A. Murphy and N. Hershkowitz
Department of Physics and Astronomy, University of Iowa, Iowa City, Iowa 52240
(Received 24 July 1972)

Mössbauer absorption spectra have been observed for Fe_2B from 290 to 1175 °K. A change in the electric quadrupole interaction was observed from 460 to 480 °K and interpreted as a result of the rotation of the easy axis of magnetization as a function of temperature. The effective magnetic hyperfine field as a function of temperature is found to be described by $(1 - T/T_C)^\beta$ in the range defined by $1.2\times10^{-3} \leq 1 - T/T_C \leq 7\times10^{-1}$ for $\beta = 0.32 \pm 0.01$. A discontinuity in the isomer shift of 0.018 ± 0.010 mm/sec was found across the ferromagnetic transition.

I. INTRODUCTION

Metallic borides of iron are part of the group of refractory hard metals consisting of the carbides, nitrides, borides, and sulfides. Their physical and chemical properties have been studied extensively by Weiss and Forrer[1] and Hägg in the 1930's[2,3] and by Kiessling in the late 1940's and early 1950's.[4,5]

More recently the iron borides have drawn interest in many areas of research. These compounds range from Fe_3B[6] to FeB_n, where n is 95 at. %.[7] FeB as well as other monoborides have been studied by Lundquist and Meyers,[8] Cooper *et al.*,[9] and others.

Fe_2B is the subject of this study. It is known to have a body-centered-tetragonal ($CuAl_2$-type) structure which is common to the metal borides with the general formula M_2B.[5] Its lattice constants taken from x-ray crystallographic data are $a = 5.109$ Å and $c = 4.249$ Å.[10]

The first studies of the ferromagnetic characteristics of Fe_2B were saturation magnetization measurements by Weiss and Forrer in 1929. More recent investigations by Cadeville and Daniel[11] and Cadeville and Meyer[12] have led to a determination of the Curie temperature of 1015 °K. Both nuclear-magnetic-resonance[13,14] and Mössbauer-effect measurements[9,15–18] have been applied to the iron-boron compounds. The results of the Mössbauer-effect investigations are summarized in Table I.

Bernas and Campbell[19] examined room-temperature Mössbauer spectra of FeCo (0 and 3 at.% V) and Fe_2B (0, 2, and 10 at.% Mn) in an attempt to determine the contribution to the hyperfine field of iron by the conduction-electron polarization. Their approach stemmed from the empirical evidence of the occurrence of what was termed "low-field satellites" when any impurity was introduced which lowered the saturation magnetization of the host. They concluded that conduction-electron polarization plays little part in the hyperfine structure of the interstitial compound Fe_2B. Also, a broadening of the high-energy lines of Fe_2B spectra was observed which they suggested was due to the electric quadrupole interactions in two inequivalent sites.

Weisman *et al.*[18] performed nuclear-magnetic-resonance and Mössbauer-effect experiments on Fe_2B and Fe_2Zr. The Mössbauer spectra were taken at 298, 77, and 4.2 °K and showed an asymmetry. They proposed that the asymmetry was due to an anisotropic magnetic hyperfine interaction similar to that studied in Fe_2Zr by Wertheim *et al.*[20] and Gegenwarth *et al.*[21] Fe_2Zr has an easy axis of magnetization which results in two magnetically inequivalent iron sites having a 3-to-1 population ratio. In the absence of a magnetic field, the iron sites in Fe_2Zr as well as in Fe_2B are crystallographically equivalent. However, in the case of Fe_2B, the existence of a magnetic axis in the c plane can result in equal numbers of two inequivalent iron positions. Their data were least-squares fitted, assuming two independent six-line hyperfine-field patterns and the results have been given in Table I and labeled sites A and B. The difference in the magnetic fields at the iron sites was about 3%.

The magnetocrystalline anisotropy of a single crystal of Fe_2B was directly measured by Iga *et al.*[22] using a torque magnetometer. The sample crystal was a disk 2.5 mm in diameter and 0.35 mm thick. The disk plane included both the a and c axes. The easy axis of magnetization was found to change continuously as a function of temperature from its position in the c plane to along the c axis. This change occurred over the temperature range 518–524 °K. This indicates that one might expect the anisotropic electric quadrupole hyperfine interactions in Fe_2B to be temperature dependent and that this could be observed using Mössbauer techniques. Also, the existence of the magnetization axis in a direction along the c axis results in the equivalence of all iron sites; thus the asymmetry observed in the room-temperature Mössbauer spectra would be expected to disappear at temperatures exceeding this point.

Also of interest is the temperature dependence of the relative magnetization. Jeffries and Hersh-

TABLE I. Summary of Mössbauer-effect data of iron boride compounds.

Compound	Hyperfine field (kOe)	Quadrupole interaction (mm/sec)	Isomer shift[a] (mm/sec)	Temperature (°K)	Ref.
Fe_2B	242 ± 10	< 0.1	0.25 ± 0.1	300	b
Fe_2B	242		0.16	300	c
FeB	118		0.28	300	c
FeB	131	0.217 ± 0.008		298	d
FeB	0	0.092 ± 0.007		622	d
Fe		0.273	0.362	300	e
(1 at. %) B		to 1.45	to 1.161	300	e
Fe_2B					
Site *A*	240 ± 2	0.05 ± 0.02	0.17 ± 0.05	298	f
Site *B*	232 ± 2	0.01 ± 0.02	0.17 ± 0.05	298	f
Site *A*	253 ± 2	0.05 ± 0.02	0.22 ± 0.05	77	f
Site *B*	243 ± 2	0.0 ± 0.02		77	f
Site *A*	252 ± 2	0.05 ± 0.02	0.23 ± 0.05	4.2	f
Site *B*	244 ± 2	0.01 ± 0.02		4.2	f

[a]Relative to iron.
[b]Reference 15.
[c]Reference 9.
[d]Reference 16.
[e]Reference 17.
[f]Reference 18.

kowitz[16] determined that in FeB the magnetic hyperfine field could be described over the region $4\times10^{-4} < 1 - T/T_C < 1.3\times10^{-1}$ by the expression $(1 - T/T_C)^{\beta}$, where $\beta = 0.545 \pm 0.010$ and $T_C = 597$ °K. Since the models describing the monoborides and semiborides are similar,[9] it is of interest to investigate the temperature dependence of the relative magnetization in Fe_2B.

II. EQUIPMENT AND EXPERIMENTAL PROCEDURE

A. Properties of Fe_2B

Fe_2B is a refractory hard-metal compound which displays metallic properties characteristic of such compounds. Some of its properties have already been discussed. It has a body-centered-tetragonal $CuAl_2$-type (C-16) crystal structure. It has lattice constants of $a = 5.109$ Å and $c = 4.249$ Å, with $c/a = 0.832$, and a density of 7.0 g/cm^3.[10] The 11 nearest iron neighbors of a typical iron atom are as follows: The closest is at 2.41 Å, two atoms are 2.44 Å distant, four sites are 2.69 Å away, and the farthest removed are the four sites at 2.72 Å. Each iron atom has twofold symmetry about one plane parallel to the c plane and one plane perpendicular to the c plane. Fe_2B is ferromagnetic with a magnetic moment of about $1.9\mu_B$ per iron ion at 20 °K. Its Curie temperature is about 1015 °K.[12]

B. Absorbers

Experiments were performed using both Fe_2B powder samples made at the University of Iowa with the facilities of the Department of Chemistry and commercial Fe_2B. The noncommercial samples were prepared using electrolytic iron and isotopically enriched B powder. It was necessary to grind the iron to a powder (about 100 mesh). Appropriate amounts of the iron and boron powder were weighed out and mixed as uniformly as possible. Then the mixture was pressed into a disk shape using a 60-ton hydraulic press. The disk-shaped sample was placed in an alumina crucible and heated to approximately 2000 °C in a radio-frequency induction furnace. The sample was then removed and ground to 300 mesh. Debye–Scherrer x-ray powder patterns were taken of all samples made to ensure their singularity of composition. The results of all powder-pattern measurements were in agreement, to within ± 0.001 Å, with published lattice parameters.

Some difficulties were encountered in maintaining stable samples at temperatures near or above the Curie temperature of 1015 °K. The samples were gradually reduced, with the subsequent appearance of free iron as an impurity. Various methods of sample containment and isolation were tried, all of which succeeded in lowering the rate of the sample reduction; however, none completely eliminated the problem. Of the techniques tried, two were used with relative success for these experiments. The first of these methods involved sandwiching the powder sample between two quartz sheets each approximately 0.5 in. square and 0.005 in. thick. The edges were cemented in a helium atmosphere with Aremco 505 alumina cement. This prevented trapping any water vapor. The sheets were ground from quartz glass using a geological vacuum-chuck grinder and the thickness gauged with a micrometer caliper. The disadvantage of this technique was that the quartz sandwich attenuated the 14.4-keV-source γ rays to such an extent that with a relatively thick powder sample the running time necessary to achieve Mössbauer spectra whose depths were greater than ten stan-

dard deviations was unreasonable (greater than 48 h). The second and preferred method employed the alumina cement as the only supporting medium. Since the castings were somewhat porous, a film of SiO was evaporated onto both sides of a sample disk. The film thickness was estimated to be approximately 1 mg/cm^2. Absorbers made in this fashion yielded attenuation of the 14.4-keV-source γ rays of typically less than 25%. This allowed count rates within the window of the single-channel analyzer of usually 200 counts/sec or greater with shields and oven vacuum jackets in place. The signal–to–signal-plus-noise ratio was typically 0.7.

C. Apparatus

The experimental configuration consisted of a conventional Mössbauer spectrometer. The radioactive source mounted to the constant-acceleration drive was ^{57}Co in a copper matrix. This drive was operated in conjunction with a multichannel analyzer and a proportional counter. A general description of this configuration has been given elsewhere.[23]

Velocity calibrations of the Mössbauer drive were obtained both from ^{57}Fe-metal-absorber Mössbauer spectra[24] and by using laser interferometry. The resulting calibrations proved to be consistent to within 1.0%.

The absorbers were contained in an electrically heated vacuum oven capable of obtaining temperatures of 1270 °K with a power input of approximately 170 W. A schematic representation is shown in Fig. 1. The oven was constructed at the University of Iowa and consisted of an aluminum vacuum jacket with 0.010-in. -thick beryllium windows, four interior titanium thermal-radiation shields, and cast-ceramic heater coils and absorber holder. Typically, temperatures in the range of 1000 °K could be maintained to within ± 0.5 °K. The measuring thermocouples were 0.015-in. -diam chromel-P–alumel. Control was accomplished either by a proportional controller or by manually varying the heater voltage.

III. DATA

Data were acquired from room temperature to approximately 1175 °K. The data can be classed into three regions of differing characteristics. The first region is characterized by a large relative magnetic hyperfine splitting and small electric quadrupole perturbation. The second region involves mixed magnetic and electric quadrupole hyperfine interactions of comparable magnitude. The final region is one of zero internal magnetic field with only electric quadrupole interactions present. Figure 2 illustrates spectra representing data taken within each of these three regions.

The Hamiltonian describing the high-magnetic-field region (region 1) is derived by Abragam.[25] In this region the energy states are determined by the magnetic hyperfine interaction and the electric quadrupole interaction is treated as a weak perturbation. The splitting of the energy levels can be

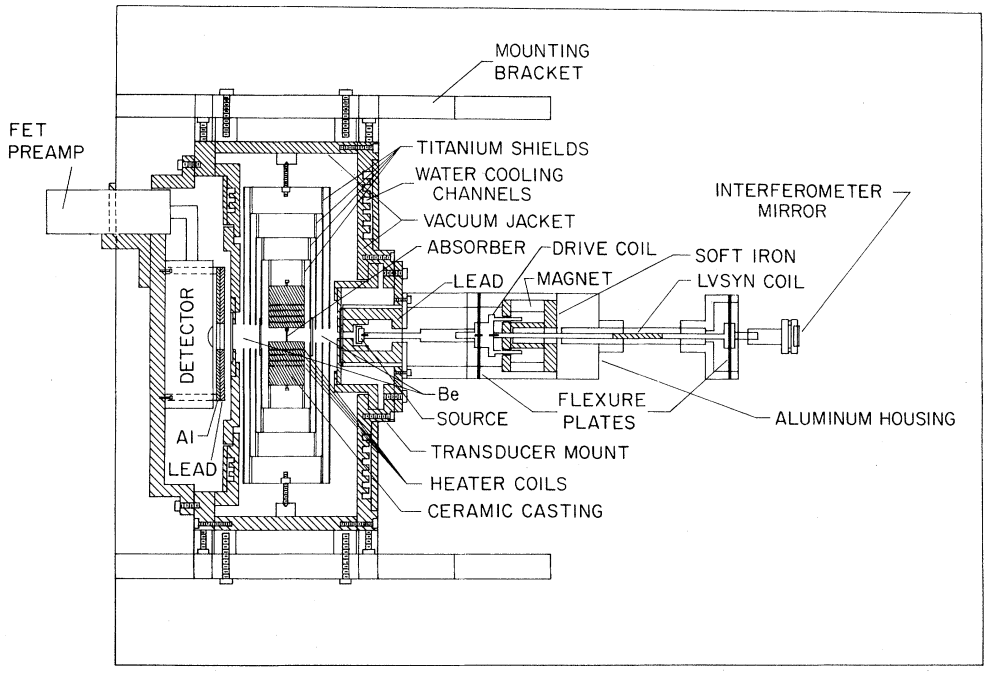

FIG. 1. Cutaway view of Mössbauer spectrometer apparatus including high-temperature vacuum oven.

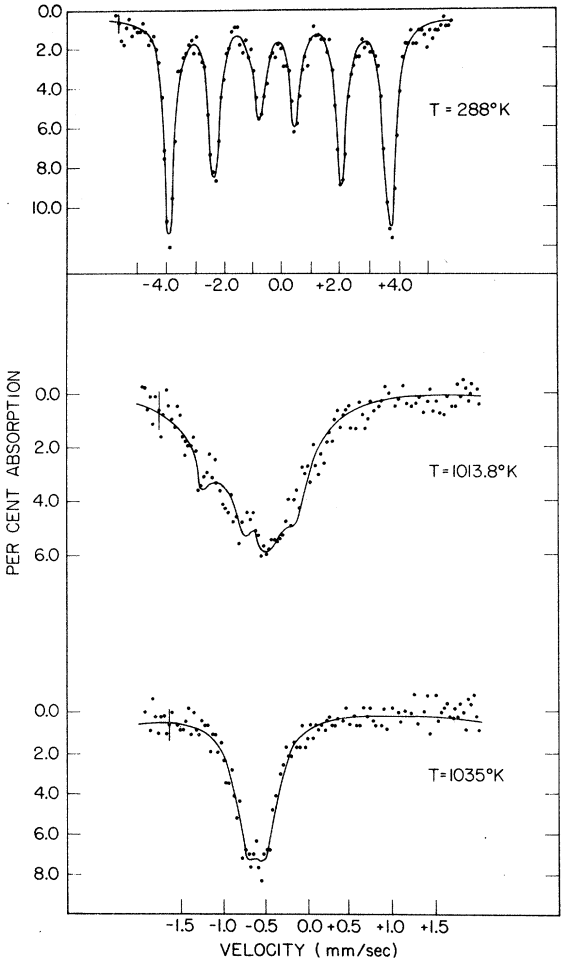

FIG. 2. Mössbauer spectra representative of Fe_2B data. Solid lines are least-squares fits to the data uncorrected for the signal-to-noise ratio.

written

$$\Delta E = -m_I g_I H + \epsilon_m \ ,$$

where

$$\epsilon_m = \frac{e^2qQ}{8I(2I-1)} \ [3m^2 - I(I+1)] \times (3\cos^2\theta - 1 + \eta \sin^2\theta \cos 2\Phi),$$

where I is the nuclear spin, g_I is the nuclear gyromagnetic ratio, and H is the effective internal magnetic field at the nucleus. The expression e^2qQ is the conventional notation for the electric quadrupole interaction. The axes are the principal axes of the electric-field-gradient tensor and are chosen such that

$$|V_{zz}| \geq |V_{yy}| \geq |V_{xx}| \ ,$$

and η is the asymmetry parameter defined by

$$\eta = (V_{xx} - V_{yy})/V_{zz} \ .$$

Then θ and Φ are the polar angles defining the direction of the z axis with respect to $\vec{H}$.

Fitting in this region was done using both 12- and 6-line routines. The 12-line fits were two superimposed 6-line hyperfine patterns of either Lorentzian or arctangent intensity shapes[26] whose linewidths, intensity ratios, and isomer shifts were constrained to be equal. The effective hyperfine field and the electric quadrupole perturbation which determined the line positions were allowed to vary independently for each six-line hyperfine-field pattern. In the six-line fitting routines, the widths of lines 1 and 6, 2 and 5, and 3 and 4 were allowed to vary independent of each other, where the line numbers signify the relative line positions on an energy scale, 1 being the lowest-energy position and 6 being the highest-energy position.

Region 3, the zero-effective-hyperfine-field region, is similarly easy to analyze. The Hamiltonian describing this region is also given by Abragam.[25] The energy eigenvalues can be written

$$E_Q = \frac{e^2qQ}{4I(2I-1)} \ [3m_I^2 - I(I+1)] \ (1 + \tfrac{1}{3}\eta^2)^{1/2},$$

where the parameters are as defined previously.

It should be noted that the sign of the quadrupole coupling is not obtained from a measurement on a polycrystalline (powder) specimen when the only interaction present is the electric quadrupole. In this case the widths and intensities were also constrained to be equal. Attempts were made to fit the data with two pairs of split lines whose electric quadrupole coupling parameters were allowed to vary independently. However, this did not improve the fit.

The data in region 2 were the most difficult to reduce for two reasons. For this case there is no closed form solution. The problem relies on solving the complete interaction Hamiltonian which can be written[25]

$$H = H_Q + H_m \ ,$$

where

$$H_Q = \frac{e^2qQ}{4I(2I-1)} \ [3I_z^2 - I(I+1) + \eta(I_x^2 - I_y^2)]$$

and

$$H_m = -g\mu_N H[I_z \cos\theta + (I_x \cos\Phi + I_y \sin\Phi) \sin\theta],$$

where the z axis is the direction of the z component of the electric field gradient, and I_x, I_y, I_z are the matrices of the angular momentum operator. The other parameters have been defined previously. Numerical solutions of this problem have been given by Parker[27] and others.

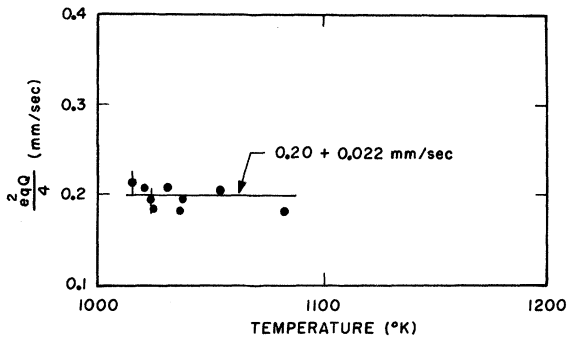

FIG. 3. Least-squares linear fit to the electric quadrupole interaction versus temperature in the region above the ferromagnetic Curie temperature.

An additional problem is that for the Fe_2B samples that were studied the linewidth is comparable to both hyperfine interactions in region 2. As the ferromagnetic Curie temperature is approached, the lines collapse on top of each other and the resolution becomes such that the lines can no longer be accurately analyzed. In this range, which for this experiment was 1000 °K, or 15 °K below the transition, to the transition temperature T_C, the information obtainable from the Mössbauer spectra was minimal. However, the width of the absorption envelope was used to accurately determine the Curie temperature T_C.

Basically two approaches were followed in reducing the Mössbauer spectra in this region. The first approach follows the procedure employed by Jeffries and Hershkowitz.[16] It involves making the assumptions of a temperature-independent electric field gradient that is axially symmetric, and the existence at each iron nucleus of a unique electric field gradient and magnetic hyperfine field. The crystal structure of Fe_2B does not have the necessary symmetry properties to require the existence of an axially symmetric electric field gradient; however, from the analysis of the data this assumption does not appear to be grossly incorrect. The value of the electric quadrupole interaction obtained for this experiment in the region of zero magnetic hyperfine field ($T > T_C$) was

$$\tfrac{1}{4}e^2qQ = 0.20 \pm 0.022 \text{ mm/sec}$$

(see Fig. 3).

The value obtained in the region where $H > 160$ kOe and above $T = 490$ °K, where the effects of the rotation of the easy axis of magnetization were observed, was

$$\tfrac{1}{4}e^2qQ[\tfrac{1}{2}(3\cos^2\theta - 1)] = -0.037 \pm 0.003 \text{ mm/sec}$$

(see Fig. 4). This yielded a value of θ of approximately 63°.

The intermediate data were then fitted so as to be consistent with the numerical calculations of Parker for that value of θ.

The second approach to reducing the data in region 2 involved the procedure described by Kündig.[28] This procedure does not necessitate the assumption of a temperature-independent axially symmetric electric field gradient. However, satisfactory fits for the data in this region were obtainable assuming $\eta = 0$. This allowed a minimum number of fitting parameters and lessened the possibilities of ambiguous results. In this routine the six-line positions were free parameters as well as the intensities. The widths were constrained to be equal. The initial-fit parameters were taken from the fits following the previously described approach. The combined use of both approaches led to a consistent interpretation of the data of this tempera-

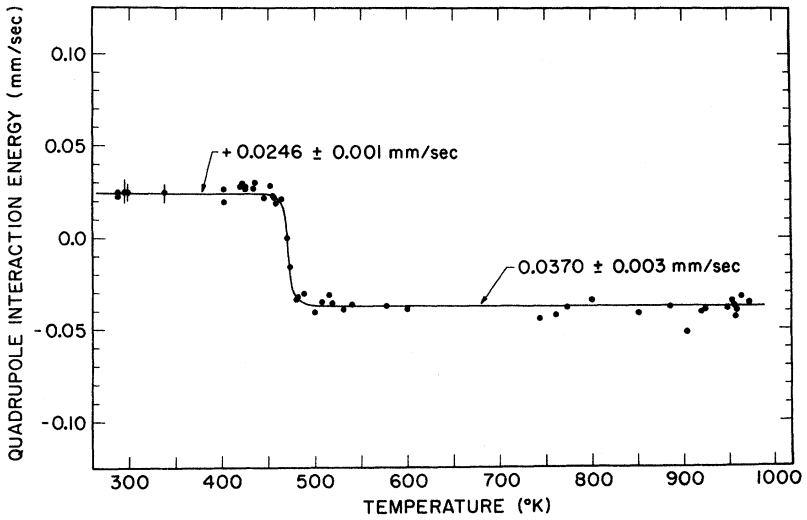

FIG. 4. Electric quadrupole interaction versus temperature in the region below the ferromagnetic Curie temperature. The straight lines are least-squares fits to the data. The smooth curve is a hand fit through the transition region.

ture region.

The parameters of interest determined from the reduction of the Mössbauer absorption spectra include the electric quadrupole interaction, effective internal magnetic hyperfine field, and isomer shift. The results were obtained from a total of 78 Mössbauer absorption spectra taken on different Fe_2B-powder-absorber samples. The error bars were determined from the computer calculations via the error-matrix routine. The graphs also include the results obtained using both arctangent and Lorentzian distributions. Only one value is plotted for both results unless they differed by an amount greater than the statistical-fit error as determined from the error-matrix calculations. The ferromagnetic Curie temperature of each of the samples was obtained relative to the temperature scales of the corresponding thermocouples used for each sample. Five different thermocouple configurations were used during this experiment. The spectra from the region of the Curie temperature and above were fitted with two single lines with fixed widths. The Curie temperature was determined as the temperature at which the displacement of the two lines relative to each other remains constant as a function of the temperature. In this manner T_C could be determined to within ± 1.5 °K. All of the temperature scales corresponding to the various thermocouple configurations were adjusted such that the determined Curie temperatures were equal.

IV. RESULTS AND DISCUSSION

The results of this experiment have led to the observation of two principal phenomena of interest. The first was a significant change in the electric quadrupole interaction as a function of temperature and the second was the temperature dependence of the effective internal magnetic hyperfine field. In addition, the temperature dependence of the isomer shift was observed.

The results of the Mössbauer spectra of Fe_2B show a large change in the electric quadrupole perturbation interaction energy that occurs at approximately 470 °K, which is shown in Fig. 4. Both the 6- and the 12-line-fit results indicate the same phenomena, although the latter has a considerably greater amount of scatter. Also the hyperfine fields of the two superimposed 6-line (12-line) fits become equivalent to within the statistical error above this temperature region. This is evidence that the iron sites are equivalent and that the easy axis does indeed lie along the c axis.

The transition region is seen to extend from approximately 460 to 480 °K. Notice that the electric quadrupole interaction energy changes sign and goes through zero as indicated by the data point at 471 °K. A least-squares straight-line fit to the six-line results gives a value of the interaction energy just below the transition region of $+0.0246 \pm 0.001$ mm/sec and just above the transition region -0.037 ± 0.003 mm/sec. The 12-line results obtained were in agreement with the results of previous authors with similarly large statistical uncertainty. The phenomenon observed could be a result of a change in the electric field gradient or could result from the θ or Φ dependence, that is, a change in the orientation of the easy axis of magnetization relative to the principal axes of the electric-field-gradient tensor.

The most probable cause of the change of sign of the electric quadrupole interaction is a change in the easy axis of magnetization as a function of temperature with the magnetization along the easy axis. This view is supported by the observations of Iga[22] in a thin crystal of Fe_2B. He observed that, constrained by his sample geometry, the easy axis of magnetization rotated from the c plane to a direction along the c axis as a function of temperature. The transition occurred within the temperature range 518–524 °K, which is a 6 °K interval. This is approximately 50 °K higher than the temperature at which the electric quadrupole interaction energy shifts as observed in the present experiment. The size of the transition-temperature interval as observed by Iga also compares in order of magnitude with that observed by the present authors (20 °K). It is believed that the temperature differences are the result of differences in the sample system. The plane of the thin crystals of Iga[22] contained the a and c crystal axes. This results in a crystalline anisotropy not present in the polycrystalline sample. It is believed that this difference in the geometrical constraints of the sample systems could account for the differences in the temperature characteristics of the transition.

The least-squares fit of the electric quadrupole interaction to a straight line below the transition results in a room-temperature value of 0.0245 ± 0.005 mm/sec. This should be compared to the literature values taken from Table I. A linear least-squares fit was also performed on the data above the ferromagnetic Curie temperature, which is shown in Fig. 3. This yielded a value of 0.200 ± 0.022 mm/sec. This result is only slightly dependent on temperature. This temperature dependence can be accounted for by the thermal expansion of the crystal. The results obtained for the spectra fits above the Curie temperature were corrected for the error introduced owing to the line overlap of the unresolved spectra according to Wender and Hershkowitz.[26]

The second major phenomenon of interest in this experiment was the temperature dependence of the effective internal magnetic hyperfine field. A rough

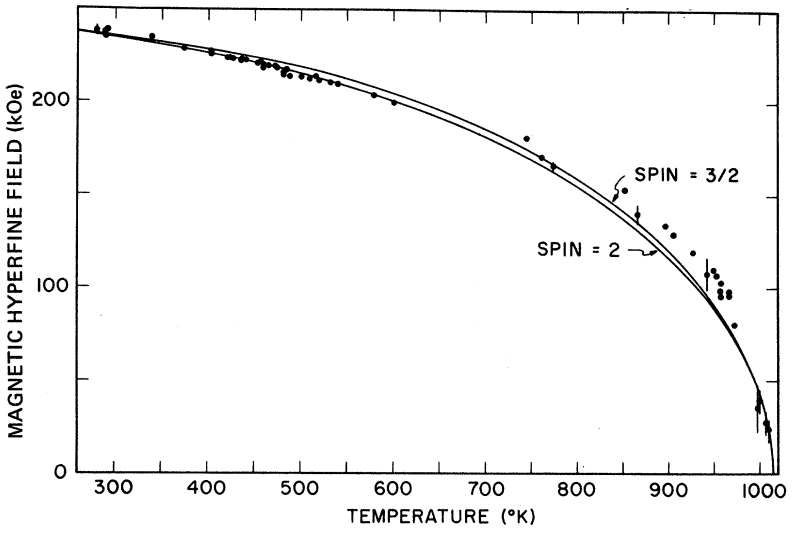

FIG. 5. Effective internal magnetic hyperfine field as a function of temperature for six-line results. The solid lines represent Brillouin functions for spins $\frac{3}{2}$ and 2.

approximation was made to the results by a Brillouin function. This is shown in Fig. 5. The closest fit is with a spin of $\frac{3}{2}$ or 2 and a saturation field of 238 kOe. The ferromagnetic Curie temperature of (1015± 1) °K is a known point which locates $H=0$.

It is generally believed that the magnetic hyperfine field near the ferromagnetic Curie temperature can be expressed by

$$H \propto (1 - T/T_C)^{\beta} ,$$

where T_C is the Curie temperature, T is the data-point temperature, and β is a constant coefficient. The value of this coefficient is predicted by different theories of ferromagnetism and ranges from $\frac{1}{3}$ to $\frac{1}{2}$.[29] Most experimental values favor $\frac{1}{3}$; however, values larger than $\frac{1}{2}$ have been obtained for Fe in Ni[30] and Fe in $YeFeO_3$.[31] The straight-line region of the plot of $\ln H$ versus $\ln(T_C - T)$ has generally been thought to be small. Jeffries and Hershkowitz,[16] however, have shown that in the case of the monoboride, FeB, the linear region was defined by

$$4.0\times10^{-4} \leq 1 - T/T_C \leq 1.3\times10^{-1} ,$$

where $T_C = 597$ °K for a value of $\beta = 0.545 \pm 0.010$.

Figure 6 is a graph of $\ln H$ versus $\ln(T_C - T)$ for the present experiment. A linear least-squares fit to all the data points is shown. The resultant slope of the straight-line fit is 0.32± 0.01 and extends over the temperature range defined by

$$1.2\times10^{-3} \leq 1 - T/T_C \leq 7.0\times10^{-1} ,$$

where $T_C = 1015$ °K.

The temperature dependence of the isomer shift

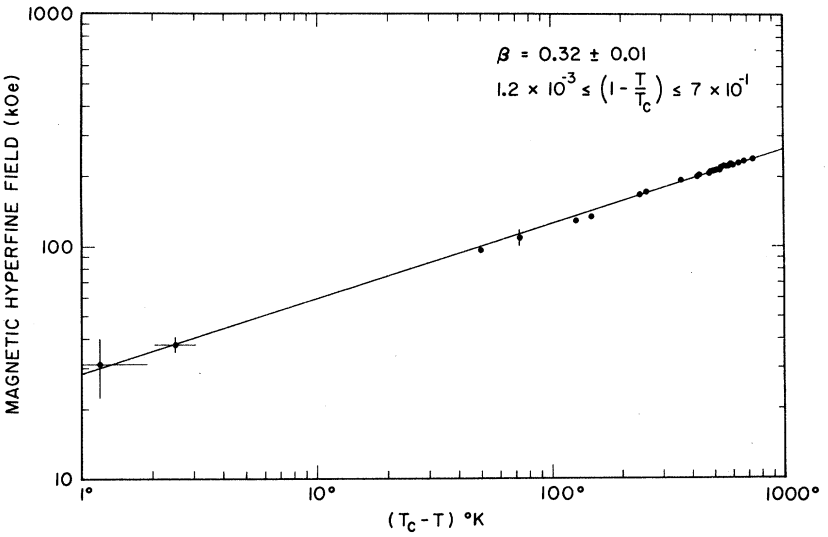

FIG. 6. A log-log plot of the effective internal magnetic hyperfine field versus $T_C - T$, where T_C = 1015 °K. The straight line represents a least-square fit to the data.

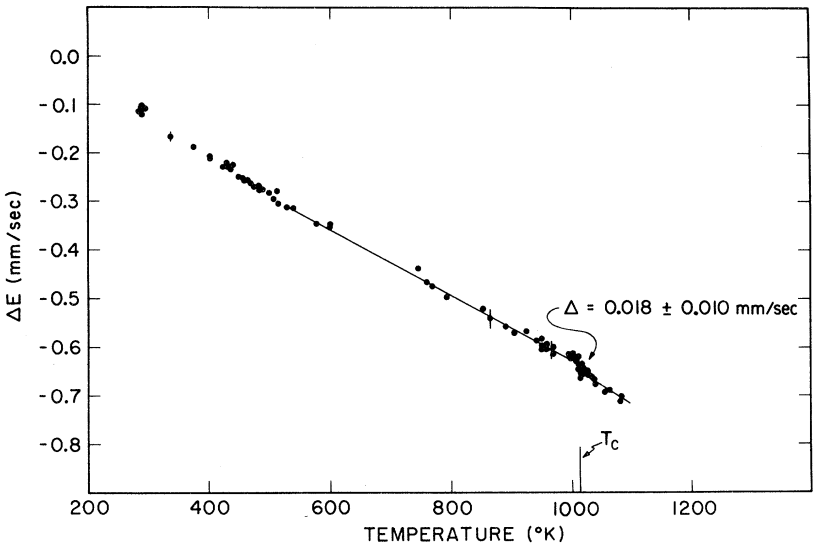

FIG. 7. Isomer shift versus temperature over the entire temperature range. The straight lines are least-squares fits to the data as shown and indicate a discontinuity at T_C.

was also observed. The results given in Fig. 7 show a discontinuity across the ferromagnetic Curie temperature of 0.018 ± 0.010 mm/sec. Examination of the isomer-shift results in the temperature region where the electric quadrupole transition takes place shows no discontinuity which is greater than the statistical error.

V. CONCLUSIONS

Mössbauer absorption spectra have been observed for Fe_2B polycrystalline samples from room temperature to 1175 °K, which is approximately 150 °K above the ferromagnetic Curie temperature. The asymmetry observed by previous investigators at room temperature becomes negligible above 500 °K. A significant change in the electric quadrupole interaction was observed at 471 °K. The temperature range of the transition was approximately 20 °K. This transition is explained by the rotation of the easy axis of magnetization as a function of temperature from its room-temperature position in the c plane to the direction along the c axis. The temperature of the electric quadrupole transition, however, was found to be approximately 50 °K below the temperature at which the easy axis has been observed to rotate by a previous author.

The effective internal magnetic hyperfine field was determined from room temperature to the ferromagnetic Curie temperature. Its temperature dependence was found to be approximated by a Brillouin function of spin $\frac{3}{2}$ or 2 and saturation magnetization of 238 kOe. The temperature dependence near the Curie temperature was found to be described by $(1 - T/T_C)^{\beta}$, where $T_C = 1015$ °K and $\beta = 0.32 \pm 0.01$ for $1.2 \times 10^{-3} \leq 1 - T/T_C \leq 7.0 \times 10^{-1}$. The isomer shift has also been determined as a function of temperature and shows a discontinuity of 0.018 ± 0.010 mm/sec across the ferromagnetic transition.

ACKNOWLEDGMENTS

The authors wish to thank Dr. E. D. Cater and Dr. N. Baenziger of the Department of Chemistry, who helped in many ways in the preparation and analysis of the polycrystalline samples. The services of the Physics Department Machine Shop is gratefully acknowledged, in particular, Alfred Scheller, Daniel Dvorsky, and Edmund Freund for their work in the construction of the apparatus for this experiment. The authors would also like to thank Stephen A. Wender for his work in developing the data-reduction programs used in this experiment.

†Work supported in part by a grant from the Research Corp.

*Research supported in part by the National Aeronautics and Space Administration, under Grant No. NGT 16-001-004, Suppl. Nos. 2 and 3.

[1]P. Weiss and R. Forrer, Ann. Phys. (Paris) 12, 279 (1929).

[2]G. Hägg, Z. Physik. Chem. B11, 152 (1930).

[3]G. Hägg, Z. Physik. Chem. 12, 413 (1931).

[4]R. Kiessling, Acta Chem. Scand. 1, 893 (1947).

[5]R. Kiessling, Acta Chem. Scand. 4, 209 (1950).

[6]A. U. Seybolt, Trans. ASM 52, 971 (1960).

[7]K. I. Portnoi, M. H. Levinskaya, and V. M. Romashov, Akad. Nauk Ukr. SSR 8, 66 (1969).

[8]N. Lundquist and H. P. Meyers, Arkiv Fysik 20, 463 (1961).

[9]J. D. Cooper, T. C. Gibb, N. N. Greenwood, and R. V. Parish, Trans. Faraday Soc. 60, 2097 (1964).

[10]W. B. Pearson, *Handbook of Lattice Spacings and Structures of Metals* (Pergamon, New York, 1967).
[11]M. C. Cadeville and E. Daniel, J. Phys. (Paris) 27, 462 (1966).
[12]M. C. Cadeville and A. J. P. Meyer, Compt. Rend. 255, 339 (1962).
[13]Hisashi Abe, Hiroshi Yasuoka, Motohiro Matsuura, Akira Hirai, and Teruya Shinjo, J. Phys. Soc. Japan 19, 1491 (1964).
[14]Hisashi Abe, Hiroshi Yasuoka, Motohiro Matsuura, Akira Shinjio, J. Phys. Soc. Japan 21, 77 (1966).
[15]T. Shinjio, F. Itoh, H. Takaki, Y. Nakamura, and N. Shikazono, J. Phys. Soc. Japan 19, 1252 (1964).
[16]J. B. Jeffries and N. Hershkowitz, Phys. Letters 30A, 187 (1969).
[17]R. Wäeppling, L. Haeggström, and S. Devanarayanan, Uppsala University (Sweden) (unpublished).
[18]I. D. Weisman, L. J. Swartzendruber, and L. H. Bennett, Phys. Rev. 177, 465 (1969).
[19]H. Bernas and I. H. Campbell, Phys. Letters 24A, 74 (1967).
[20]G. K. Wertheim, *Mössbauer Effect: Principles and Applications* (Academic, New York, 1964).
[21]R. E. Gegenwarth, J. I. Budnich, S. Skalski, and J. H. Wernick, J. Appl. Phys. 37, 1244 (1966).
[22]Atsushi Iga, Y. Tawara, and A. Yanase, J. Phys. Soc. Japan 21, 404 (1966).
[23]L. D. Flansburg and N. Hershkowitz, J. Appl. Phys. 41, 4082 (1970).
[24]J. J. Spijkerman, J. R. DeVoe, and J. C. Travis, Natl. Bur. Std. (U.S.) Spec. Publ. 260-20 (U.S. GPO, Washington, D.C., 1970).
[25]A. Abragam, *The Principles of Nuclear Magnetism* (Oxford U. P., London, 1961).
[26]S. Wender and N. Hershkowitz, Nucl. Instr. Methods 98, 105 (1972).
[27]P. M. Parker, J. Chem. Phys. 24, 1096 (1956).
[28]W. Kündig, Nucl. Instr. Methods 48, 219 (1967).
[29]P. P. Craig, R. C. Perisho, R. Segman, and W. A. Steyert, Phys. Rev. 138, 1460 (1965).
[30]J. G. Dash, O. Dunlap, and D. G. Howard, Phys. Rev. Letters 15, 525 (1965).
[31]G. Gorodetsky, S. Shtrikman, and D. Treves, Solid State Commun. 4, 628 (1966).

PHYSICAL REVIEW B VOLUME 7, NUMBER 1 1 JANUARY 1973

Free-Induction-Decay Shapes in a Dipolar-Coupled Rigid Lattice of Infinite Nuclear Spins

S. J. Knak Jensen and O. Platz
Department of Physical Chemistry, Aarhus University, 140 *Langelandsgade*, 8000 *Aarhus C*, *Denmark*
(Received 18 September 1972)

A molecular-dynamics experiment is used to derive free-induction-decay curves for a rigid cubic lattice with 216 classical spins coupled by magnetic dipole interaction. Free-induction-decay curves are obtained for the magnetic field along the [100], [110], and [111] axes of the lattice. The shapes of these curves are compared to the shapes derived from the expansion theory of Gade and Lowe and to the shapes based on Abragam's trial function. A considerable difference is found between the predictions of the Gade and Lowe theory and our experiments, whereas Abragam's trial functions reproduce the experiments quite well except for long times. Continuous-wave spectra obtained by Fourier transformation of the free-induction-decay curves are also reported as well as their first few moments. The moments are in good agreement with the second and fourth moments given by Van Vleck.

I. INTRODUCTION

The free-induction decay (FID) of the transverse magnetization in a dipolar-coupled rigid lattice is a fundamental problem in magnetic resonance and in the theory of many-body interactions. Until now no theory has been presented which covers the diversity of FID experiments. Lowe and Norberg[1] (LN) first calculated the FID for a system of identical particles with spin $I=\frac{1}{2}$, obtaining a good agreement with the FID experiments on CaF_2 and with the Fourier transform of Bruce's[2] continuous-wave (cw) spectra. The theory is based on an expansion procedure which has been challenged[3,4] since its convergence properties are not known and since it is not unique.

In 1966 Gade and Lowe[5] (GL) generalized the LN theory to arbitrary spin and calculated FID shapes and cw spectra for a simple cubic (sc) lattice, a face-centered-cubic (fcc) lattice, and a body-centered-cubic (bcc) lattice with spin $I=\frac{1}{2}$, 1, $\frac{3}{2}$, and ∞. Their set of equations (13)–(16) (hereafter referred to as GLI) constitute one of the most general expressions for the FID shapes of a single-ingredient-spin system published until now. Since the expression GLI is rather complicated, an approximation is always used in numerical calculations. We shall refer to this approximation [Eq. (17) in Ref. 5] as GLII. For spin$\frac{1}{2}$ GLII is identical to the LN expansion.

Another theoretical approach is that of Ewans and Powles[6] and of Lee, Tse, Goldburg, and Lowe.[7] Both groups consider the exchange term in the truncated dipolar Hamiltonian as a perturbation to the Ising term and use perturbation theory to obtain the FID. This method has been developed